

SUPPLEMENTARY MATERIAL

Anti-inflammatory effect and mechanism of action of ellagic acid-3,3',4-trimethoxy-4'-*O*- α -L-rhamnopyranoside isolated from *Hopea parviflora* in lipopolysaccharide-stimulated RAW 264.7 macrophages

B. Prabha,^a S. Sini,^b T. S. Priyadarshini,^a P. Sasikumar,^a Greeshma Gopalan,^a Jayesh P Joseph,^c M. M. Jithin,^c V.V. Sivan,^c P. Jayamurthy^{b, d*} and K. V. Radhakrishnan^{a, d*†}

^a*Chemical Sciences and Technology Division, CSIR-National Institute for Interdisciplinary Science and Technology, Thiruvananthapuram-695019, India*

^b*Agroprocessing and Technology Division, CSIR-National Institute for Interdisciplinary Science and Technology, Thiruvananthapuram- 695019, India*

^c*M. S. Swaminathan Research Foundation-Community Agrobiodiversity Centre (MSSRF- CABc), Puthurvayal, Wayanad, India*

^d*Academy of Scientific and Innovative Research (AcSIR), Thiruvananthapuram-695019, India.*

Phytochemical investigation of the stem bark of *Hopea parviflora* resulted in the isolation of **9** compounds; which includes friedelin (**1**), friedelin-3 β -ol (**2**), (-)-ampelopsin A (**3**), (-)- ε -viniferin (**4**), (-)-hopeaphenol (**5**), vaticaphenol A (**6**), 2,4,8-trihydroxyphenanthrene-2-*O*-glucoside (**7**), ellagic acid-3,3',4-trimethoxy-4'-*O*- α -L-rhamnopyranoside (**8**) and β -sitosterol- β -D-glucoside (**9**). Among them, compounds **1**, **2**, **6**, **7**, **8** and **9** are isolated for the first time from this species. Further, we evaluated the anti-inflammatory activity of compounds **4**, **5**, **6**, **7** and **8**. In this study, compound **8** inhibited the activity of proinflammatory mediators like NO, TNF- α , IL-6, 5-LOX and COX-2, also promoted the action of anti-inflammatory mediator like IL-10 *via* inhibition of the NF- κ B pathway in LPS-stimulated RAW 264.7 macrophages.

Keywords: *Hopea parviflora*; Dipterocarpaceae; ellagic acid-3,3',4-trimethoxy-4'-*O*- α -L-rhamnopyranoside; anti-inflammatory effect

CONTENTS

Experimental	4
Figure S1. ^1H NMR spectrum (500 MHz, CDCl_3) of friedelin (1)	6
Figure S2. ^{13}C NMR spectrum (125 MHz, CDCl_3) of friedelin (1)	6
Figure S3. ^1H NMR spectrum (500 MHz, CDCl_3) of friedelan-3 β -ol (2)	7
Figure S4. ^{13}C NMR spectrum (125 MHz, CDCl_3) of friedelan-3 β -ol (2)	7
Figure S5. ^1H NMR spectrum (500 MHz, Acetone- d_6) of (-)-ampelopsin A (3)	8
Figure S6. ^{13}C NMR spectrum (125 MHz, Acetone- d_6) of (-)-ampelopsin A (3)	8
Figure S7. ^1H NMR spectrum (500 MHz, Acetone- d_6) of (-)- ε -viniferin (4)	9
Figure S8. ^{13}C NMR spectrum (125 MHz, Acetone- d_6) of (-)- ε -viniferin (4)	9
Figure S9. ^1H NMR spectrum (500 MHz, Acetone- d_6) of (-)-hopeaphenol (5)	10
Figure S10. ^{13}C NMR spectrum (125 MHz, Acetone- d_6) of (-)-hopeaphenol (5)	10
Figure S11. ^1H NMR spectrum (500 MHz, Acetone- d_6) of vaticaphenol A (6)	11
Figure S12. ^{13}C NMR spectrum (125 MHz, Acetone- d_6) of vaticaphenol A (6)	11
Figure S13. ^1H NMR spectrum (500 MHz, Acetone- d_6) of 2, 4, 8-trihydroxyphenanthrene-2- <i>O</i> -glucoside (7)	12
Figure S14. ^{13}C NMR spectrum (125 MHz, Acetone- d_6) of 2, 4, 8-trihydroxyphenanthrene-2- <i>O</i> -glucoside (7)	12
Figure S15. ^1H NMR spectrum (500 MHz, $\text{DMSO-}d_6$) of ellagic acid-3,3',4-trimethoxy-4'- <i>O</i> - α -L-rhamnopyranoside (8)	13
Figure S16. ^{13}C NMR spectrum (125 MHz, $\text{DMSO-}d_6$) of ellagic acid-3,3',4-trimethoxy-4'- <i>O</i> - α -L-rhamnopyranoside (8)	13
Figure S17. ^1H - ^1H COSY NMR spectrum (500 MHz, $\text{DMSO-}d_6$) of ellagic acid-3,3',4-trimethoxy-4'- <i>O</i> - α -L-rhamnopyranoside (8)	14
Figure S18. HMQC NMR spectrum (125 MHz, $\text{DMSO-}d_6$) of ellagic acid-3,3',4-trimethoxy-4'- <i>O</i> - α -L-rhamnopyranoside (8)	14
Figure S19. HMBC spectrum (125 MHz, $\text{DMSO-}d_6$) of ellagic acid-3,3',4-trimethoxy-4'- <i>O</i> - α -L-rhamnopyranoside (8)	15
Figure S20. DEPT 135 spectrum (125 MHz, $\text{DMSO-}d_6$) of ellagic acid-3,3',4-trimethoxy-4'- <i>O</i> - α -L-rhamnopyranoside (8)	15
Figure S21. HRESIMS spectrum of ellagic acid-3,3',4-trimethoxy-4'- <i>O</i> - α -L-rhamnopyranoside (8)	16

Figure S22. ^1H NMR spectrum (500 MHz, $\text{DMSO-}d_6$) of β -sitosterol- β -D-glucoside (**9**) **16**

Figure S23. ^{13}C NMR spectrum (125 MHz, $\text{DMSO-}d_6$) of β -sitosterol- β -D-glucoside (**9**) **17**

Figure S24. Cytotoxic effect of compounds **4-8** in RAW 264.7 macrophages **17**

Figure S25. Effect of 1 μM and 5 μM concentrations of compound **8** on NO production in LPS-stimulated RAW 264.7 cell lines. Values are mean \pm SD, n = 3. $P < 0.05$. **18**

Figure S26. Effect of 1 μM and 5 μM concentrations of compound **8** on TNF- α , IL-6, 5-LOX, COX-2 and IL10 production in LPS-stimulated RAW 264.7 cell lines. Values are mean \pm SD, n = 3. $P < 0.05$ vs positive control **18**

Figure S27. Western blot analysis for the expression of NF- κ B in RAW 264.7 macrophages **19**

References **19**

Experimental

Plant material

The stem bark of *Hopea parviflora* Bedd. was collected from the Western Ghats region of Wayanad District, Kerala, India in April 2015. The plant material was authenticated by plant taxonomist of M. S. Swaminathan Research Foundation, India and a voucher specimen (**M.S.S.H. 1481**) is deposited in the Herbarium of repository of the same institute.

Extraction and isolation of phytochemicals

The air-dried and grounded stem bark of the *Hopea parviflora* (750 g) was extracted successively with *n*-hexane (2.5 L x 72 h x 3 times), acetone (2.5 L x 72 h x 3 times), ethanol (2.5 L x 72 h x 3 times) and water (2.5 L x 72 h x 3 times). The supernatant liquid was decanted, filtered and the filtrate was concentrated under reduced pressure in a rotary vacuum evaporator (Heidolph, Germany) to remove the residual solvent, which yielded 750 mg of *n*-hexane, 90 g of acetone, 24 g of ethanol and 10 g of aqueous extracts. An aliquot of acetone extract (60 g) was subjected to column chromatographic separation on silica gel (100-200 mesh, 2 L column) by *n*-hexane/ethyl acetate gradient (100% *n*-hexane to 100% EtOAc) to afford twenty fraction pools (FrA.1-FrA.20).

Fraction pool 2 (FrA.2) further subjected to column chromatography over silica gel (100-200 mesh) using 5% EtOAc in *n*-hexane, followed by crystallization by *n*-hexane and EtOAc mixture, to yielded compound **1** (5 mg) and compound **2** (8 mg) as colourless crystals. The fraction pool 5 (FrA.5) was again purified by silica gel (100-200 mesh) column chromatography by *n*-hexane-EtOAc gradient (1: 1) to afforded compound **3** (4 mg) as brown amorphous solid. The fraction pool 6 (FrA.6) was further subjected to purification on silica gel column chromatography [100-200 mesh; *n*-hexane-EtOAc (2: 3)] to yielded compound **4** (22 mg) as brown amorphous solid. The fraction pool 8 (FrA.8) was purified by precipitation method by chloroform to yielded compound **5** (3 g) as pale yellow amorphous solid. Fraction pool 9 (FrA.9) on column chromatography separation using silica gel 100-200 mesh (EtOAc-*n*-hexane) and Sephadex LH 20 (MeOH) resulted in the isolation of compound **6** (18 mg) as brown amorphous solid. Fraction pool (FrA.10) was purified by silica gel CC (100-200 mesh) with *n*-hexane-EtOAc (3:7) gradient to yielded compound **7** (14 mg) as brown amorphous solid. Fraction pool 13 was subjected to column chromatographic (silica gel 100-200 mesh) separation by *n*-hexane-EtOAc mixture (1:4) to afford compound **8** (64 mg) as

colourless amorphous solid. From the fraction pool 15, compound **9** (6 mg) was precipitated out.

Cell culture and treatment conditions

RAW 264.7 macrophages were procured from NCCS, Pune, India and were maintained in DMEM containing 10% FBS and 1% antibiotic–antimycotic mix at 37 °C in humidified air containing 5% CO₂.

Cytotoxicity assay

In order to find out the working concentration, the cytotoxicity was evaluated using MTT assay with different concentrations (1 μ M, 5 μ M, 10 μ M, 25 μ M, 50 μ M and 100 μ M) of the compounds **4-8** (Mosmann et al. 1983).

Determination of NO production

After pre-incubation of RAW 264.7 cells (2×10^6 cells/mL) with different concentrations of compound **8** and LPS (10 μ g/mL) for 24 h, the quantity of nitrite accumulated in the culture medium was measured as an indicator of NO production. Briefly, 100 μ L of Griess reagent (1% sulfanilamide and 0.1% naphthylethylenediamine dihydrochloride in 2.5% phosphoric acid), was mixed with an equal volume of cell supernatant, the mixture was incubated at RT for 10 min, and the absorbance at 540 nm was measured in a microplate reader (Moshage et al. 1995). The quantity of nitrite was determined based on a sodium nitrite standard calibration curve. Here, dexamethasone (DXM) was used as a positive control.

ELISA of TNF- α , IL-6, 5-LOX, COX-2 and IL-10

Concentrations of TNF- α (ab100747), IL-6 (ab100712), 5-LOX (ab210574), COX-2 (ab210574) and IL-10 (ab100697) in the culture medium were determined using respective ELISA kits according to the manufacturer's protocol and the absorbance was measured at the respective wavelength using microplate reader (Biotek ELX 800).

Western blot expression study

Expression level of NF- κ B was evaluated by Western blotting (Burnette et al. 1981).

Statistical analysis

Statistical analysis has done by using Graph Pad prism software. Unpaired Student's t test was carried out to test the difference between two sets of data. “P<0.05” was considered to be statistically significant.

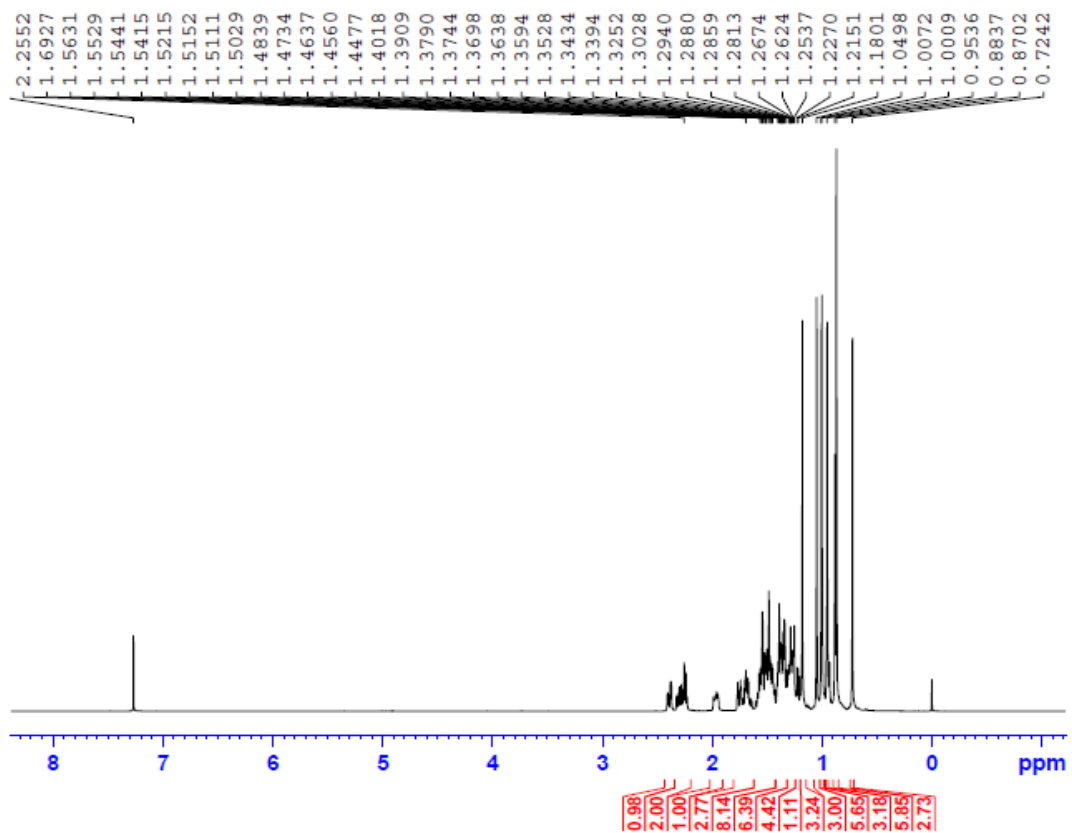


Figure S1. ^1H NMR spectrum (500 MHz, CDCl_3) of friedelin (**1**)

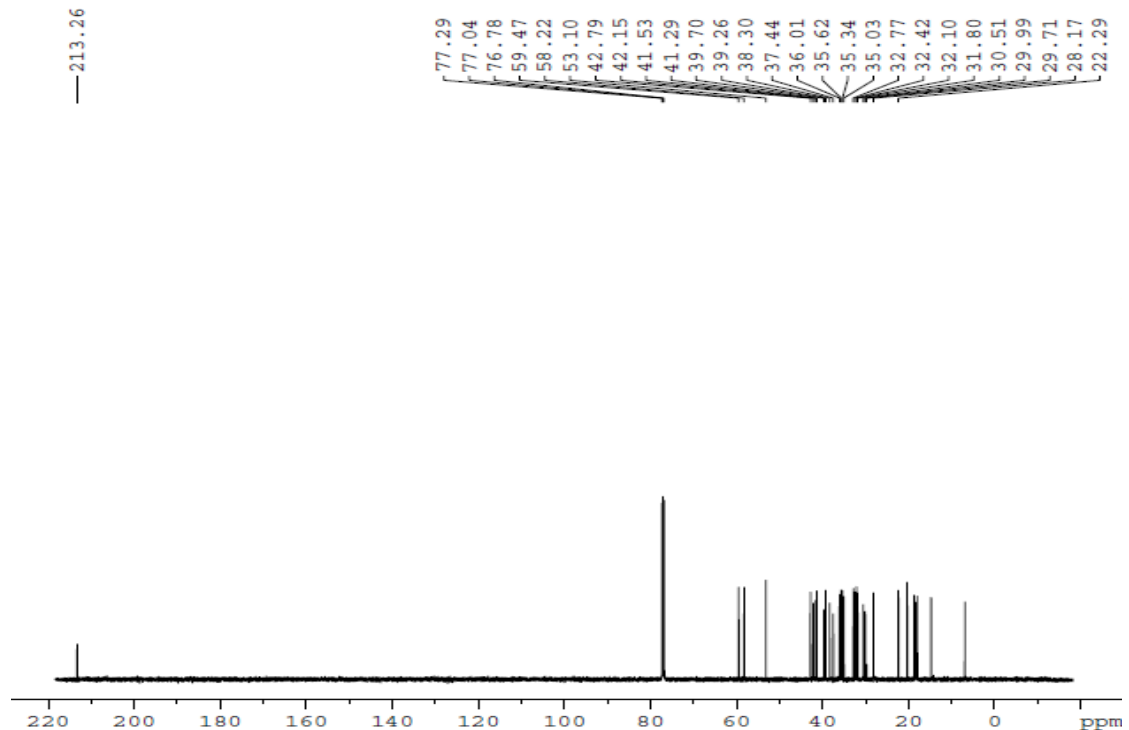


Figure S2. ^{13}C NMR spectrum (125 MHz, CDCl_3) of friedelin (**1**)

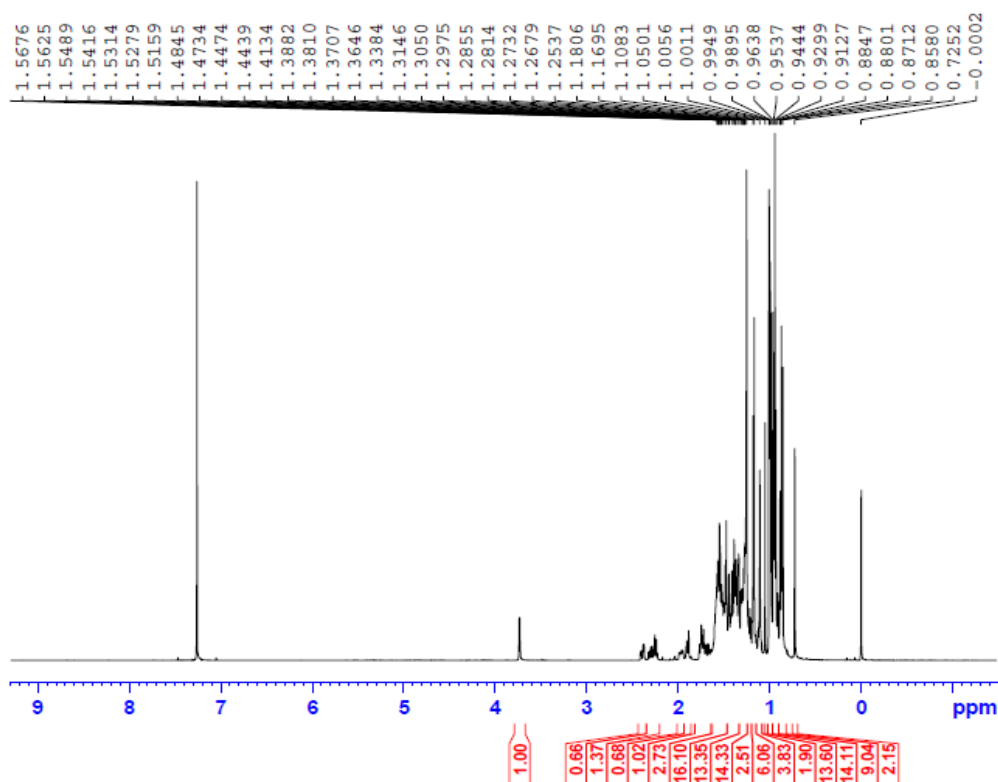


Figure S3. ^1H NMR spectrum (500 MHz, CDCl_3) of friedelan-3 β -ol (**2**)

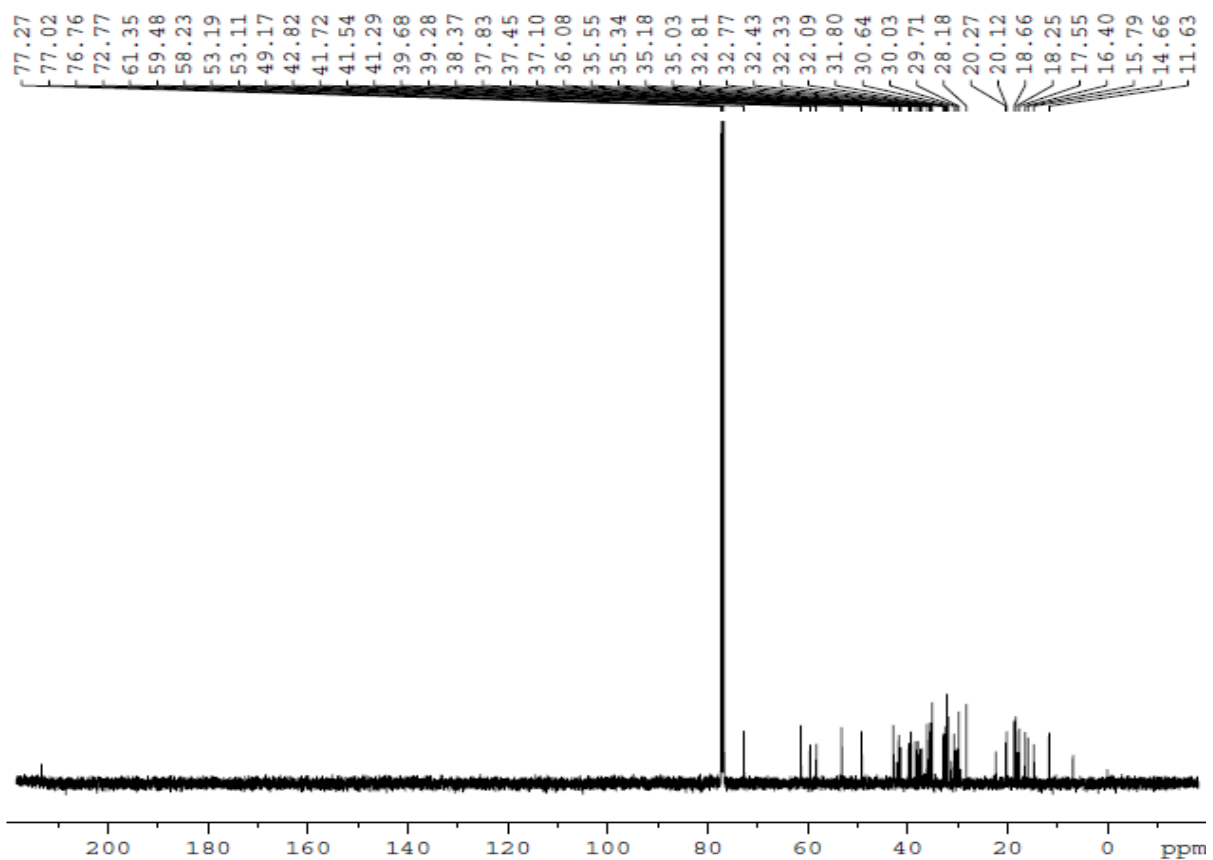


Figure S4. ^{13}C NMR spectrum (125 MHz, CDCl_3) of friedelan-3 β -ol (**2**)

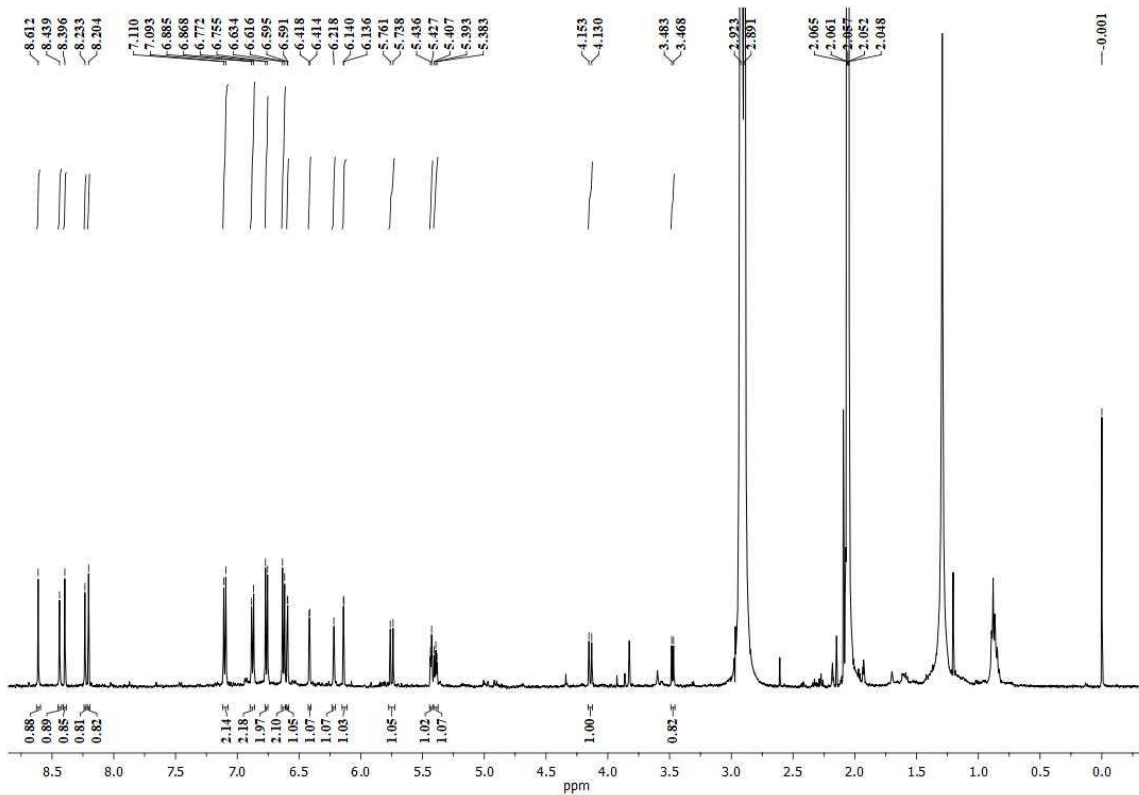


Figure S5. ^1H NMR spectrum (500 MHz, Acetone- d_6) of (-)-ampelopsin A (3)

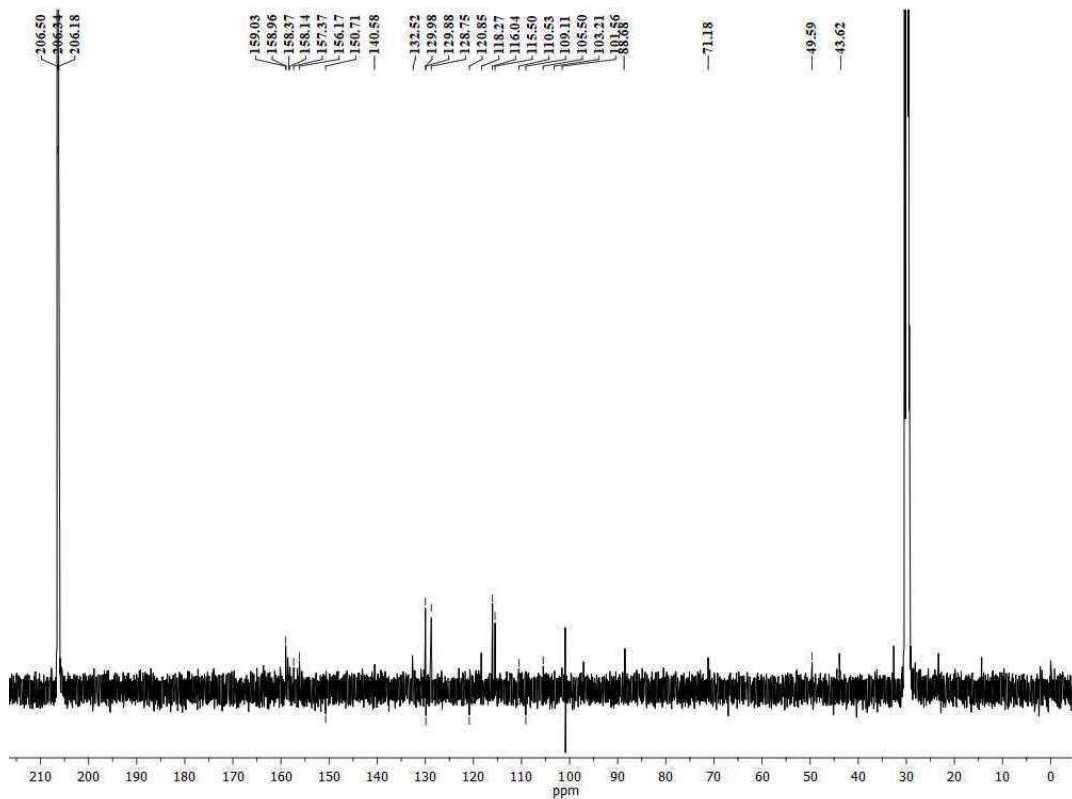


Figure S6. ^{13}C NMR spectrum (125 MHz, Acetone- d_6) of (-)-ampelopsin A (3)

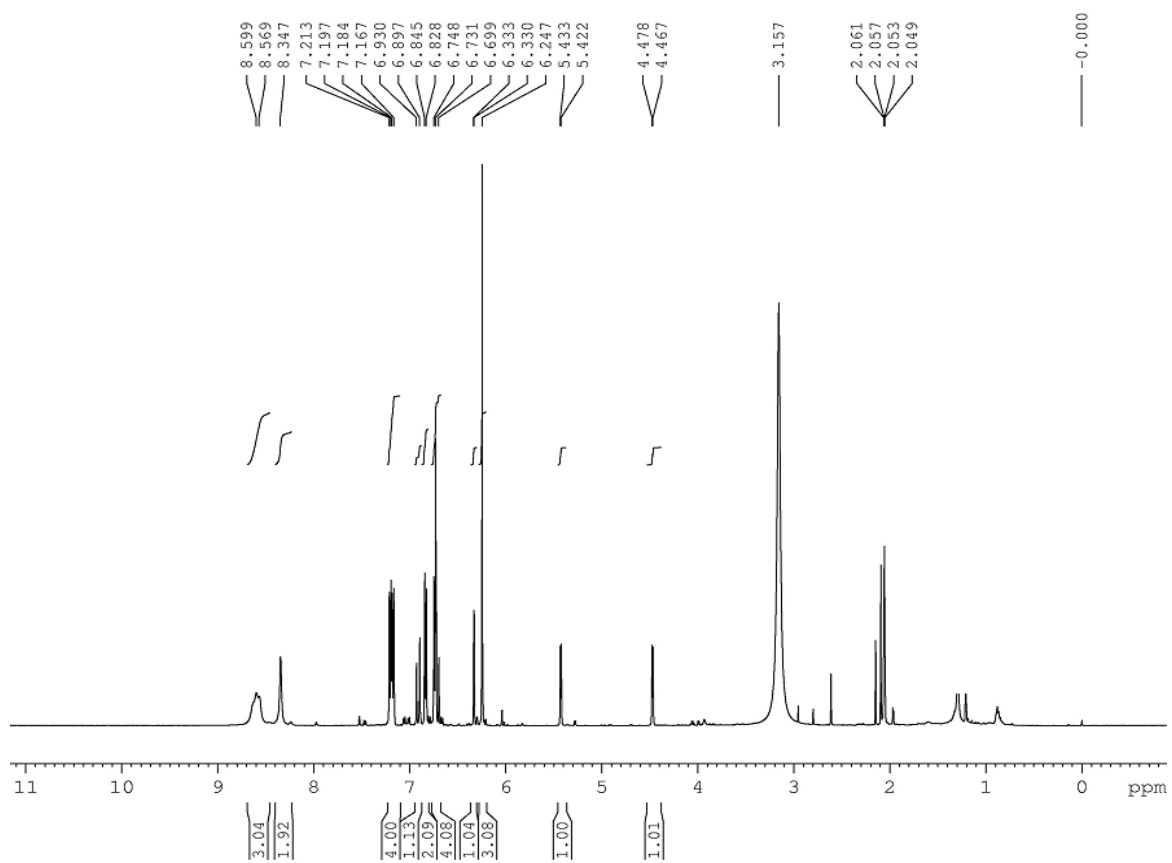


Figure S7. ^1H NMR spectrum (500 MHz, Acetone- d_6) of (-)- ε -viniferin (**4**)

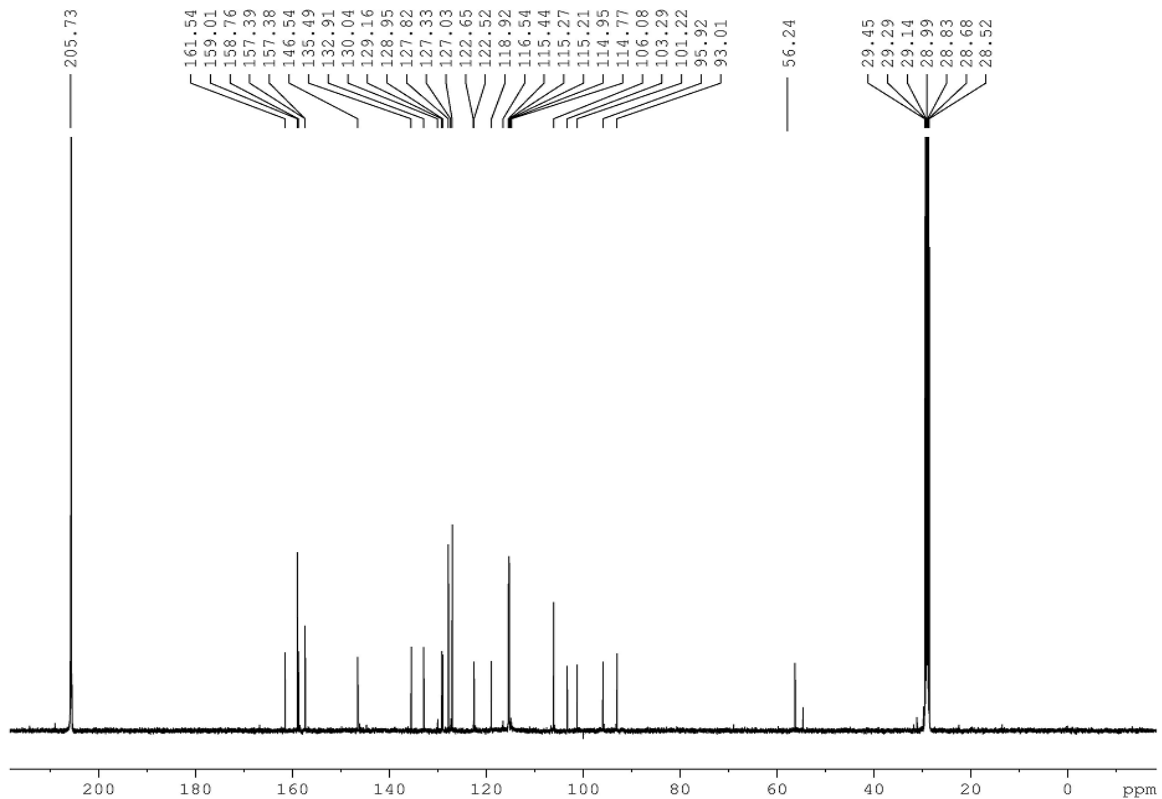


Figure S8. ^{13}C NMR spectrum (125 MHz, Acetone- d_6) of (-)- ε -viniferin (**4**)

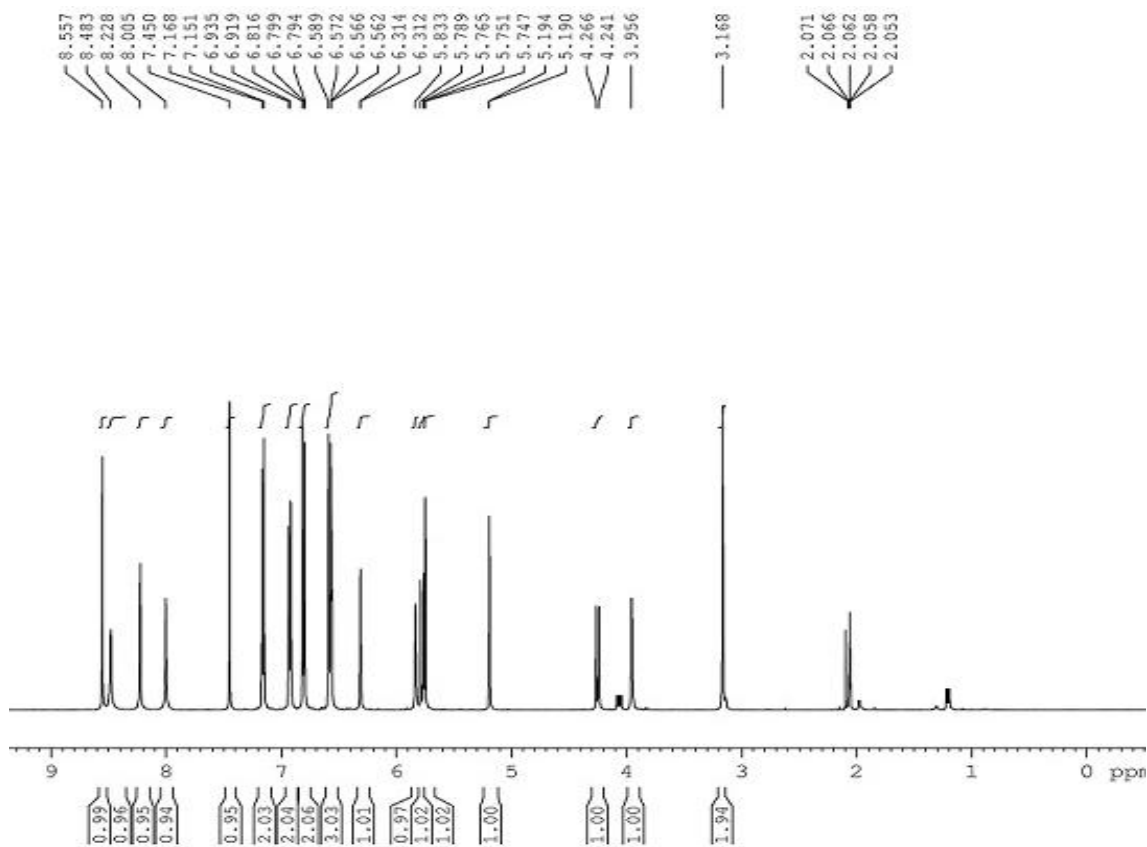


Figure S9. ^1H NMR spectrum (500 MHz, Acetone- d_6) of (-)-hopeaphenol (**5**)

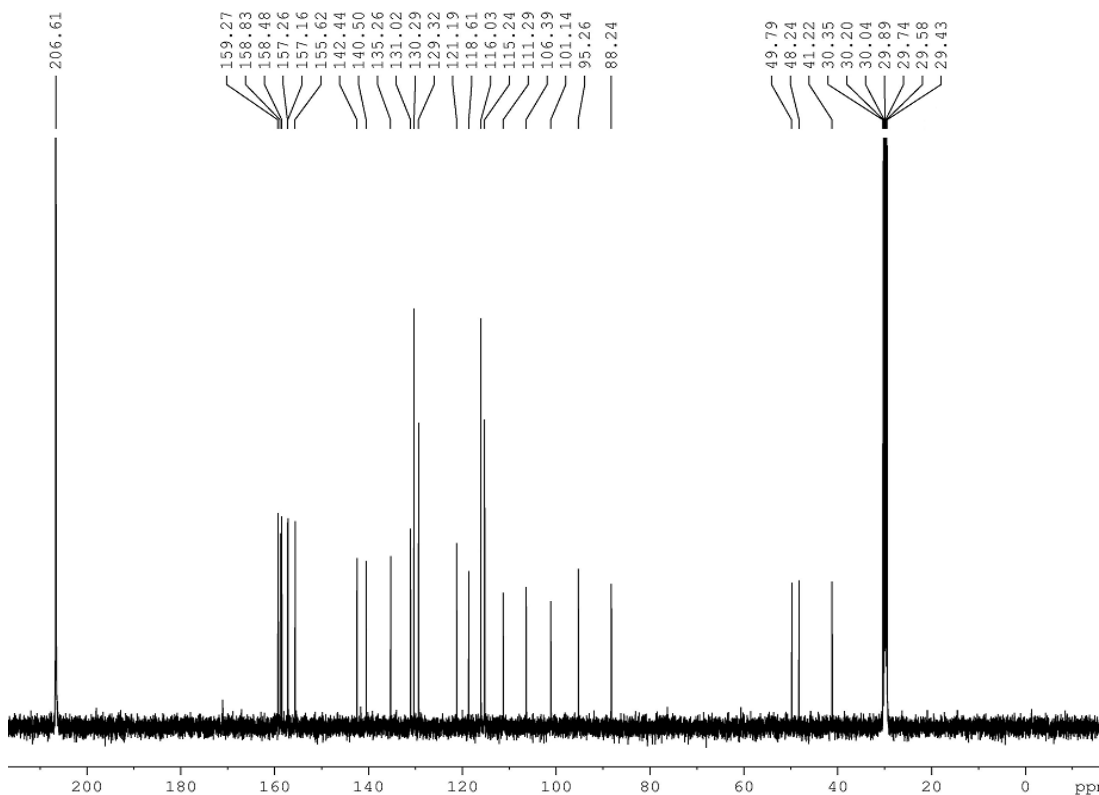


Figure S10. ^{13}C NMR spectrum (125 MHz, Acetone- d_6) of (-)-hopeaphenol (**5**)

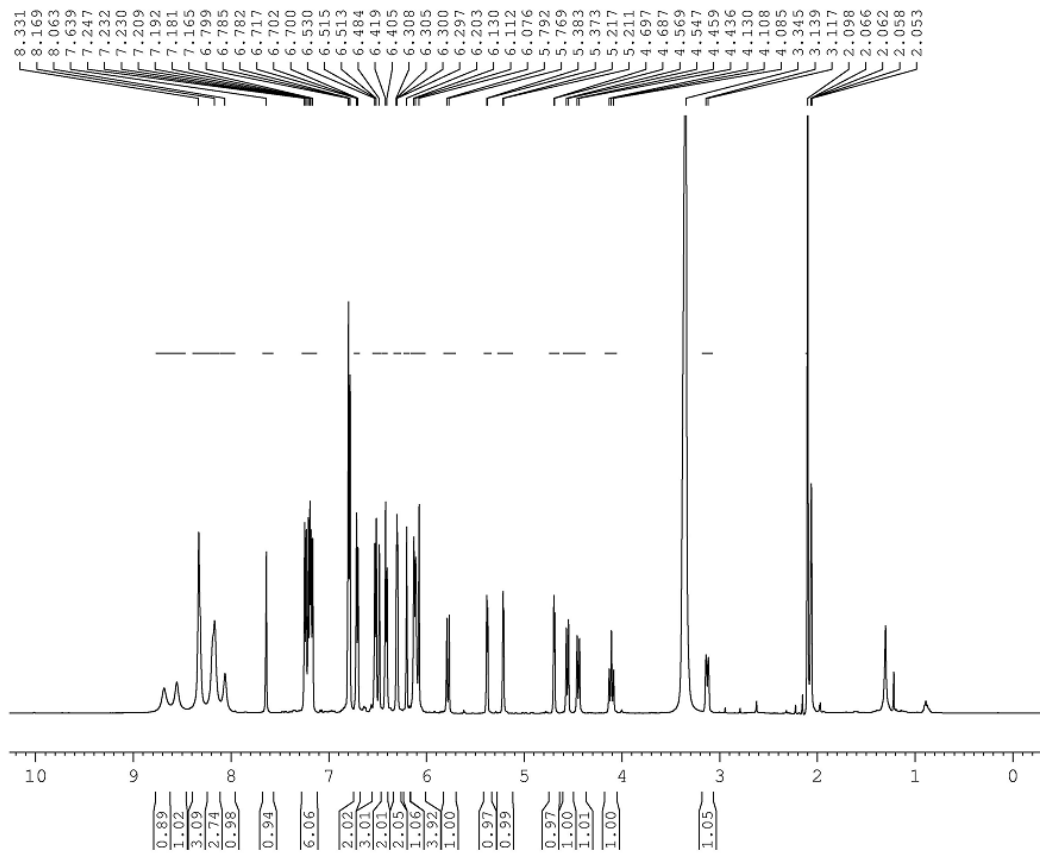


Figure S11. ^1H NMR spectrum (500 MHz, Acetone- d_6) of vaticaphenol A (**6**)

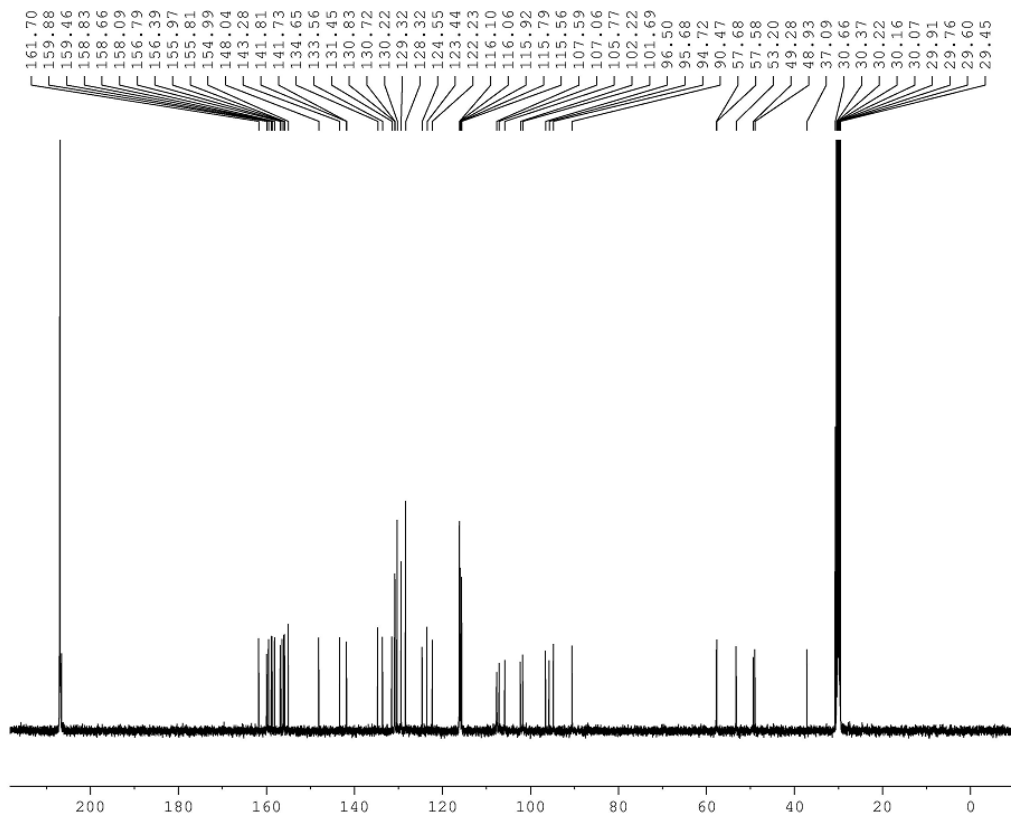


Figure S12. ^{13}C NMR spectrum (125 MHz, Acetone- d_6) of vaticaphenol A (**6**)

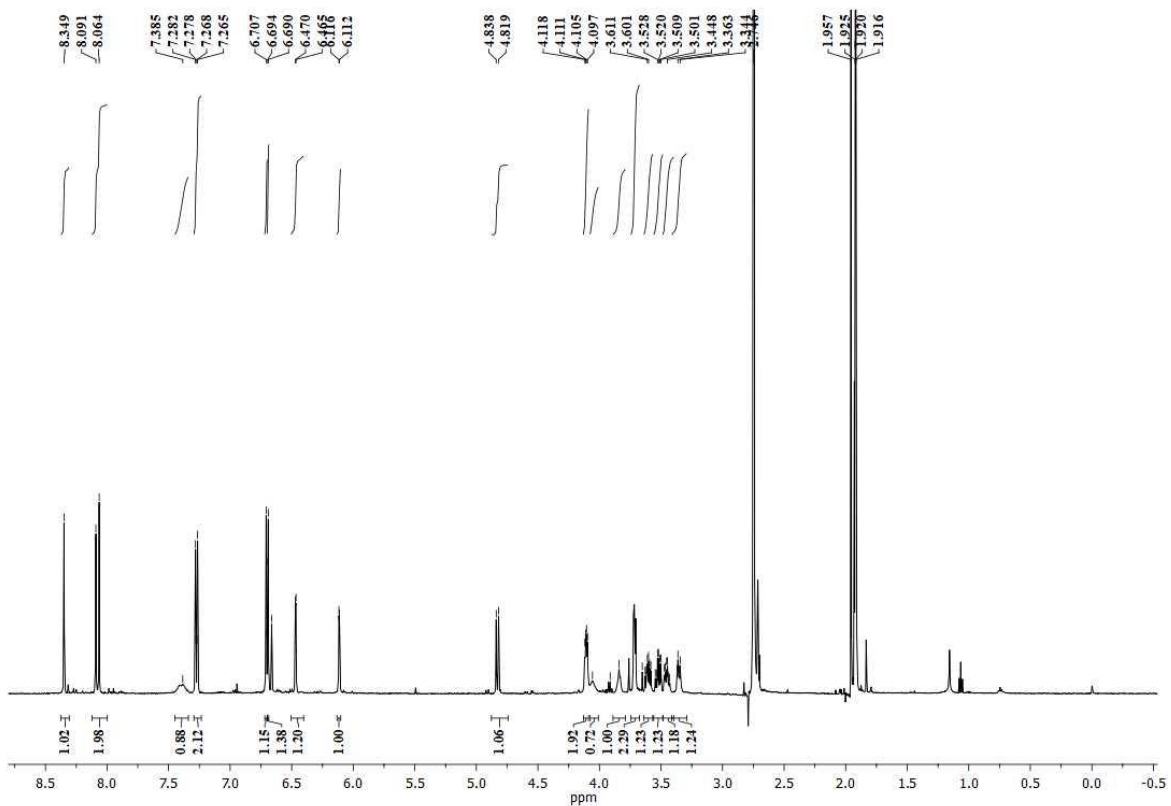


Figure S13. ^1H NMR spectrum (500 MHz, Acetone- d_6) of 2, 4, 8-trihydroxyphenanthrene-2-*O*-glucoside (**7**)

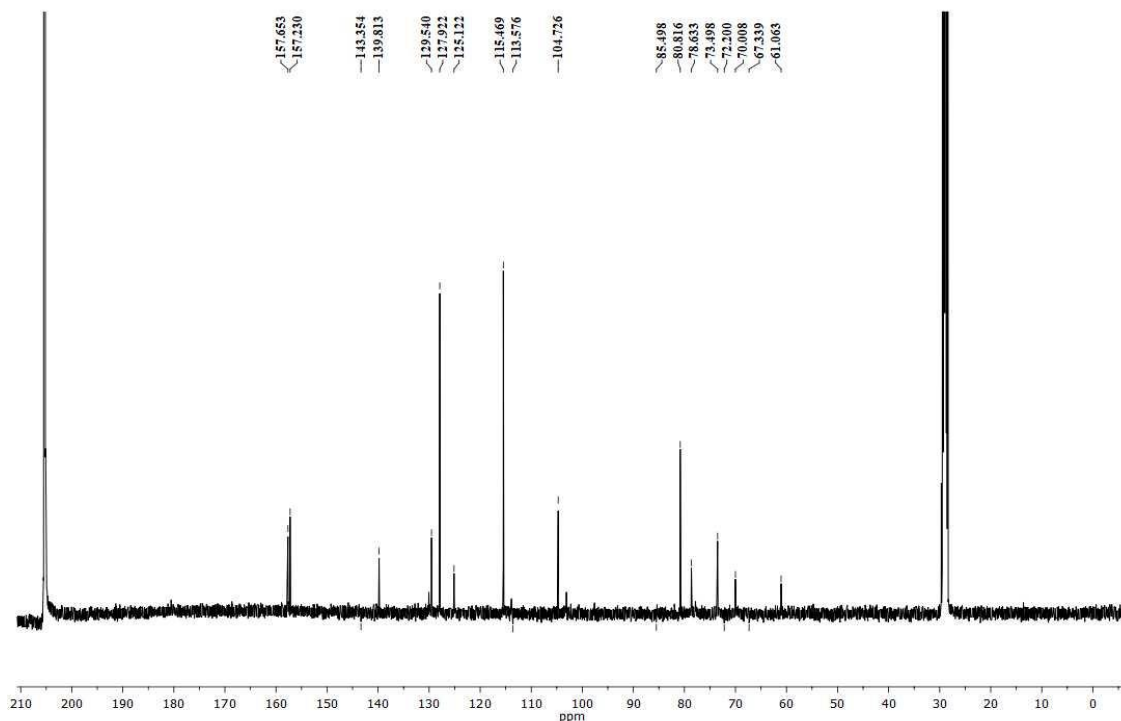


Figure S14. ^{13}C NMR spectrum (125 MHz, Acetone- d_6) of 2, 4, 8-trihydroxyphenanthrene-2-*O*-glucoside (**7**)

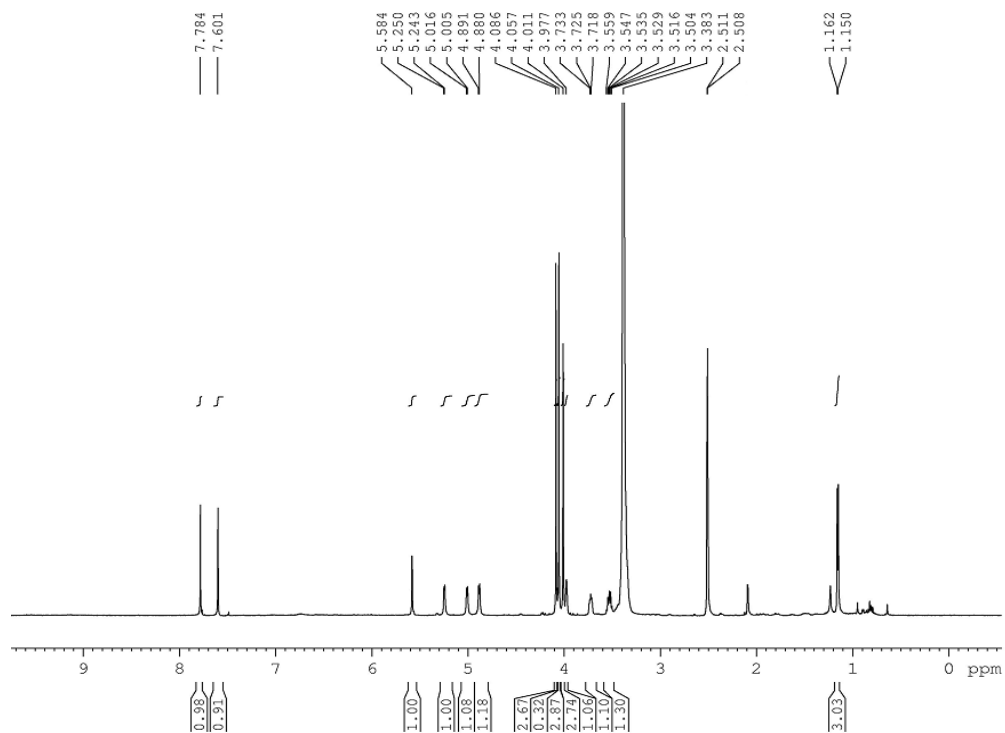


Figure S15. ^1H NMR spectrum (500 MHz, $\text{DMSO}-d_6$) of ellagic acid-3,3',4-trimethoxy-4'- O - α -L-rhamnopyranoside (**8**)

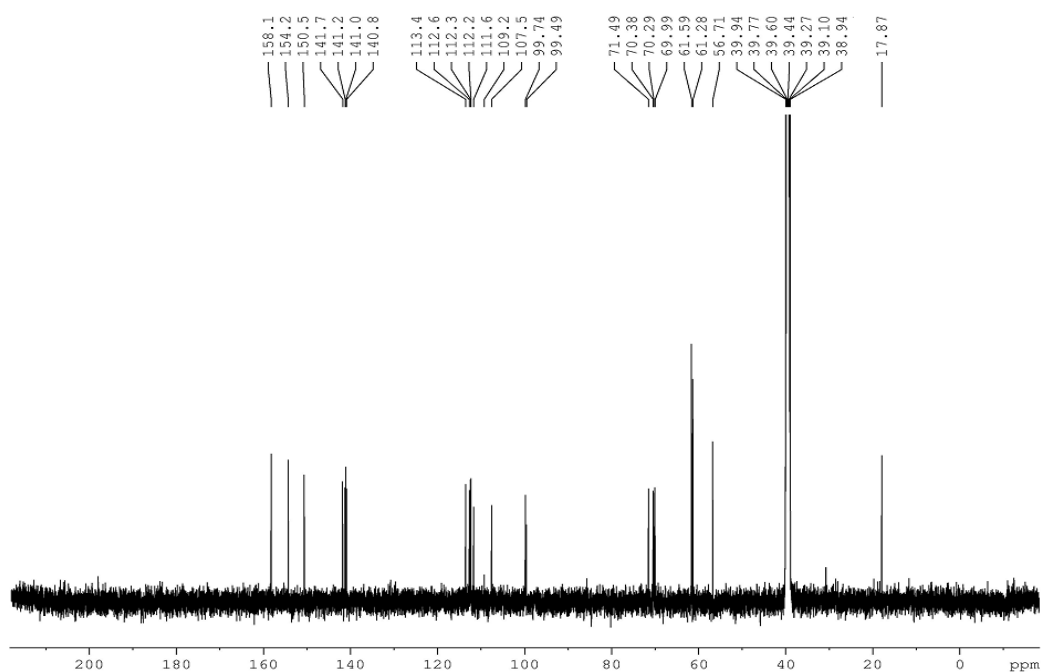


Figure S16. ^{13}C NMR spectrum (125 MHz, $\text{DMSO}-d_6$) of ellagic acid-3,3',4-trimethoxy-4'- O - α -L-rhamnopyranoside (**8**)

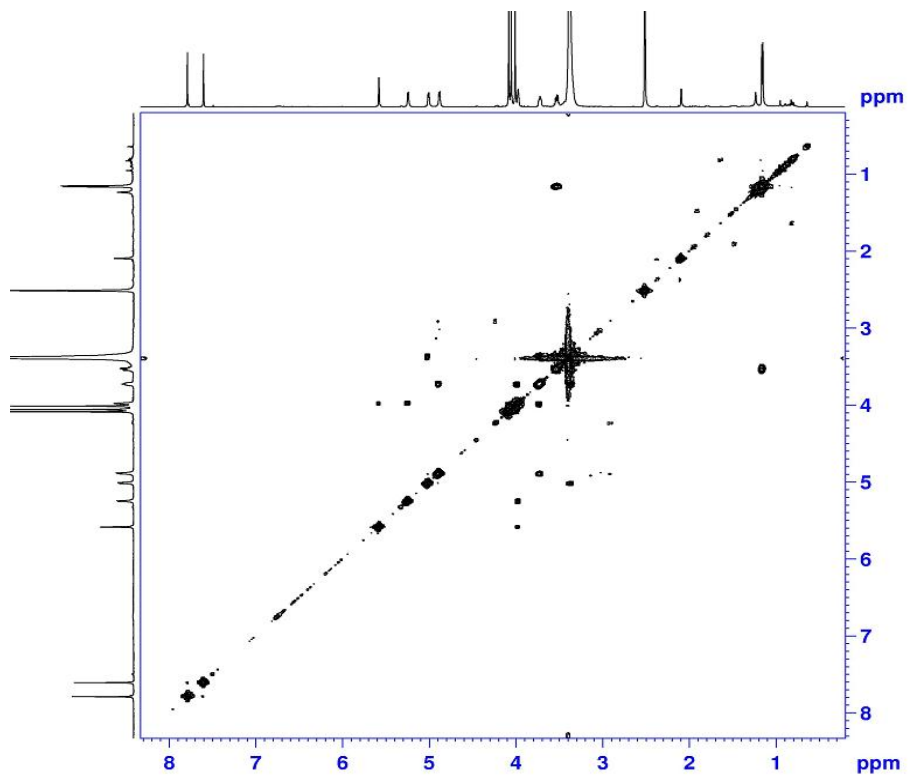


Figure S17. ^1H - ^1H COSY NMR spectrum (500 MHz, $\text{DMSO-}d_6$) of ellagic acid-3,3',4-trimethoxy-4'- O - α -L-rhamnopyranoside (**8**)

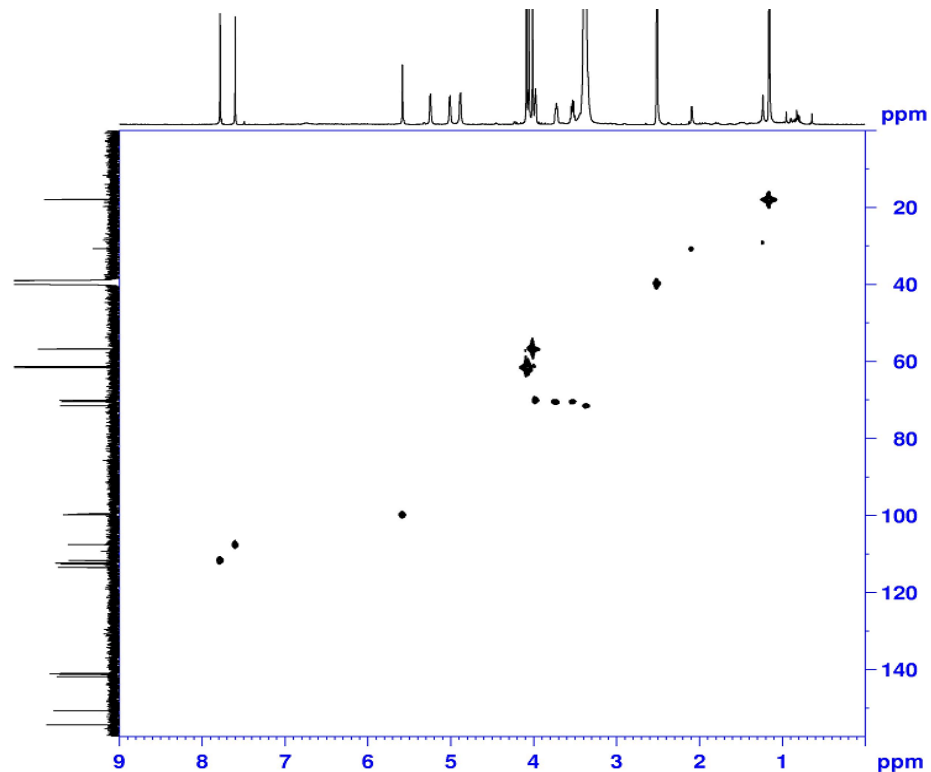


Figure S18. HMQC NMR spectrum (125 MHz, $\text{DMSO-}d_6$) of ellagic acid-3,3',4-trimethoxy-4'- O - α -L-rhamnopyranoside (**8**)

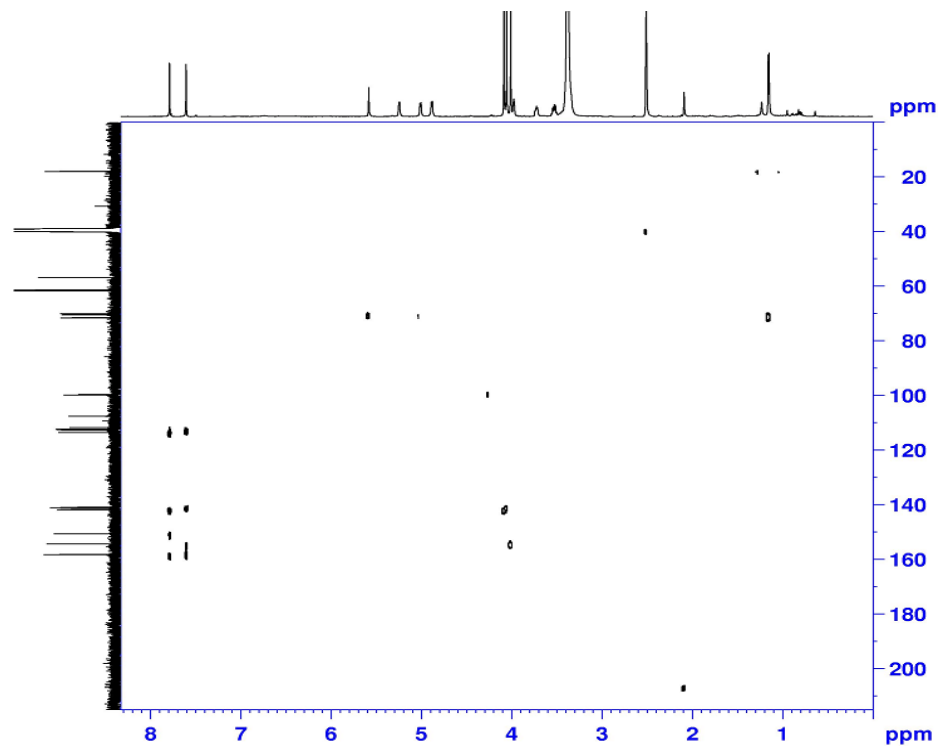


Figure S19. HMBC spectrum (125 MHz, DMSO-*d*₆) of ellagic acid-3,3',4-trimethoxy-4'-*O*- α -L-rhamnopyranoside (**8**)

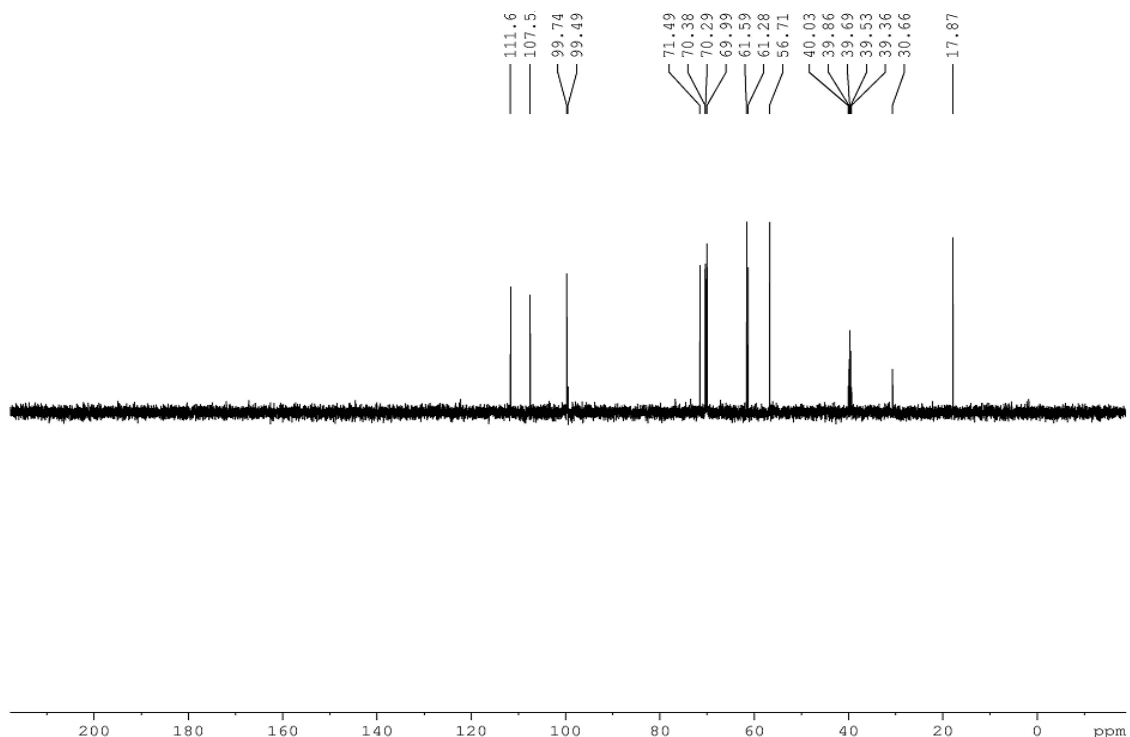


Figure S20. DEPT 135 spectrum (125 MHz, DMSO-*d*₆) of ellagic acid-3,3',4-trimethoxy-4'-*O*- α -L-rhamnopyranoside (**8**)

PB-UJ-HP-6_151029150911 #63 RT: 0.94 AV: 1 SB: 121 0.14-1.95 NL: 4.60E5
I: FTMS {1,1} + p ESI Full lock ms [80.00-1000.00]

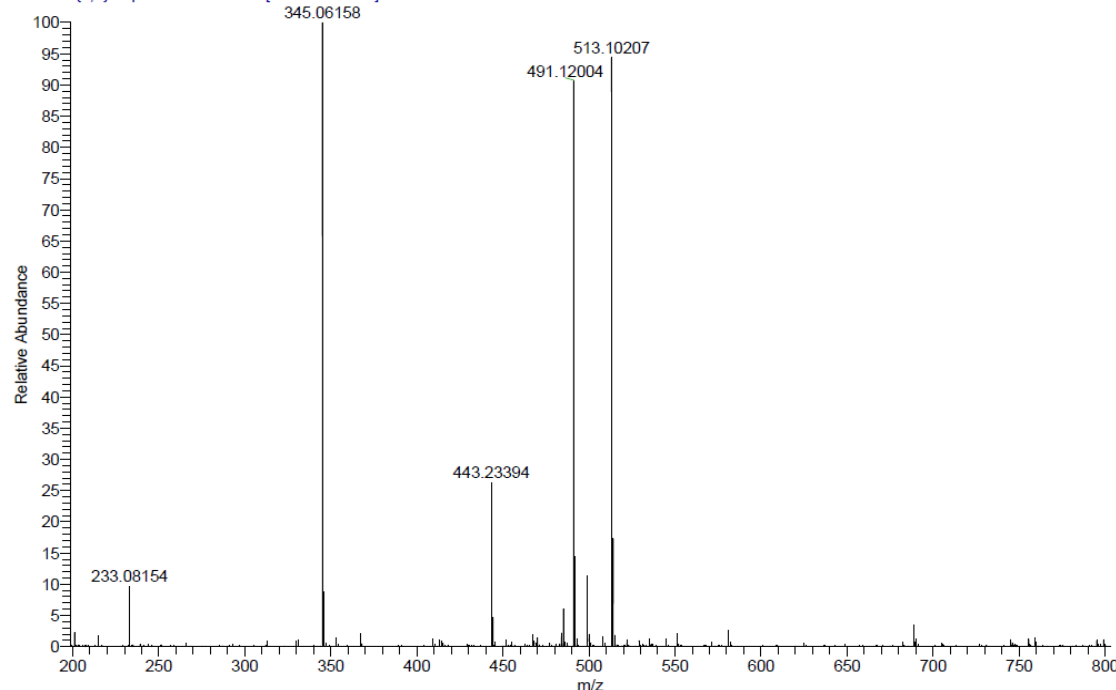


Figure S21. HRESIMS spectrum of ellagic acid-3,3',4-trimethoxy-4'-O- α -L-rhamnopyranoside (**8**)

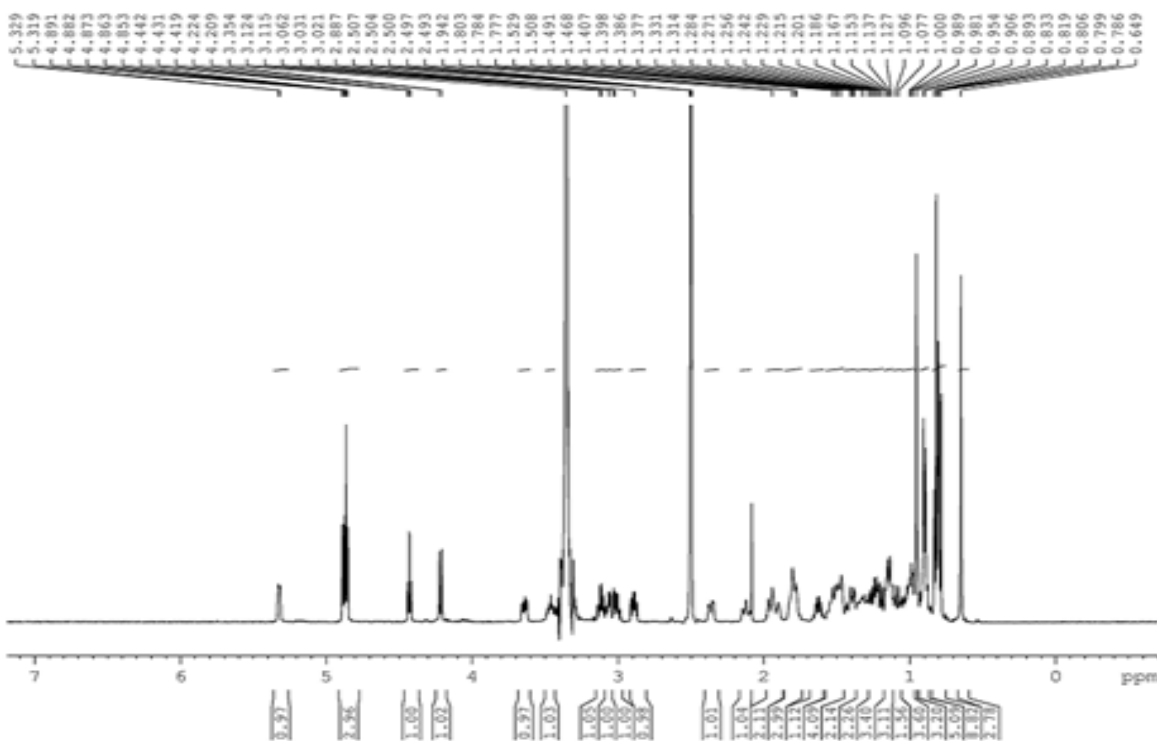


Figure S22. ^1H NMR spectrum (500 MHz, DMSO- d_6) of β -sitosterol- β -D-glucoside (**9**)

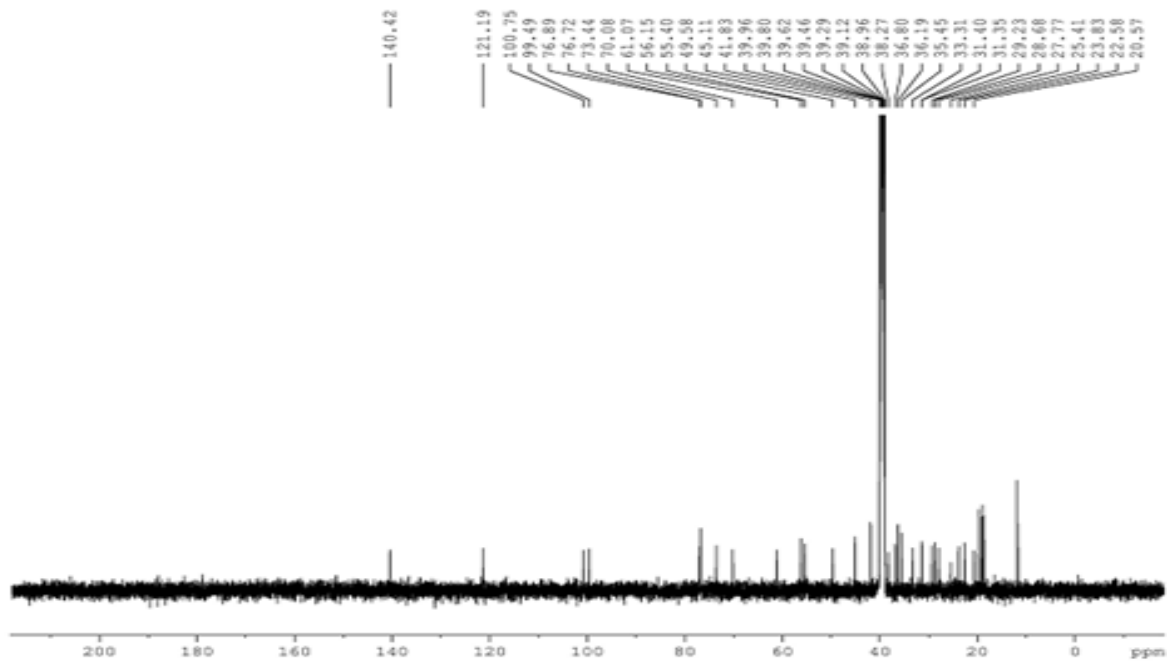


Figure S23. ^{13}C NMR spectrum (125 MHz, $\text{DMSO-}d_6$) of β -sitosterol- β -D-glucoside (**9**)

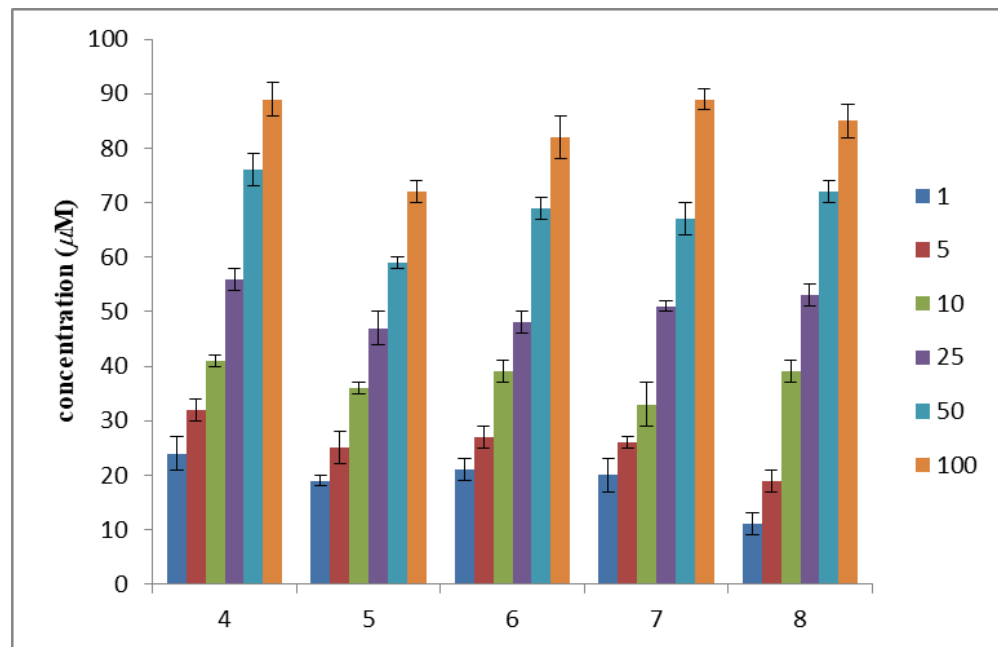


Figure S24. Cytotoxic effect of compounds **4-8** in RAW 264.7 macrophages

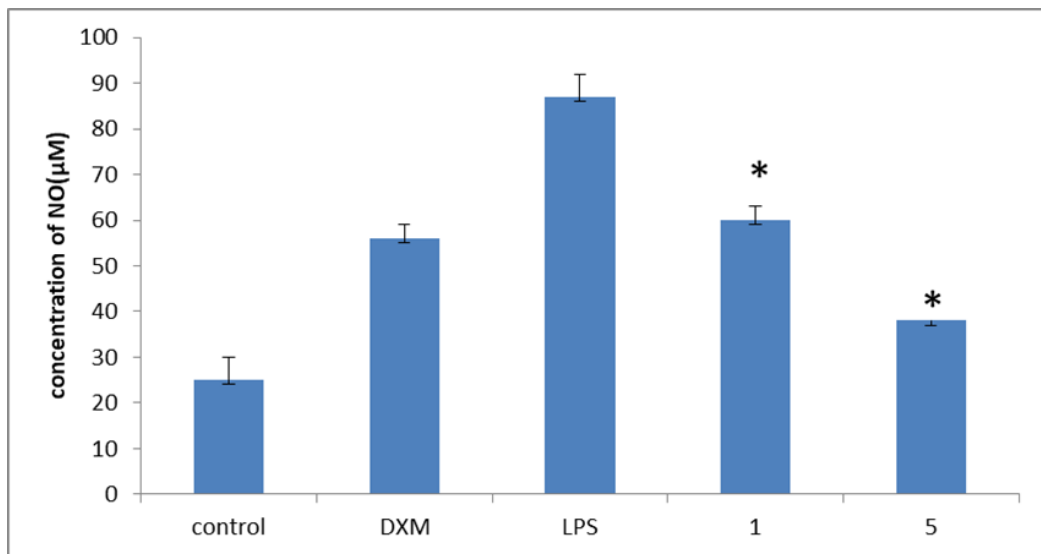


Figure S25. Effect of $1 \mu\text{M}$ and $5 \mu\text{M}$ concentrations of compound **8** on NO production in LPS-stimulated RAW 264.7 cell lines. Values are mean \pm SD, $n = 3$. $P < 0.05$.

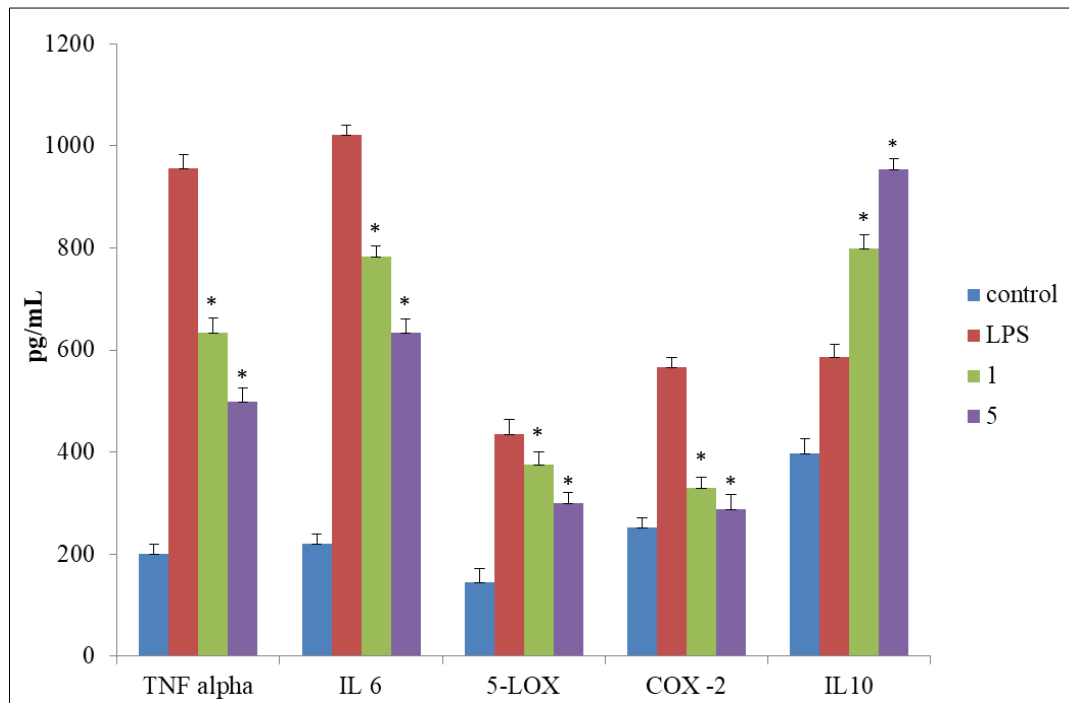


Figure S26. Effect of $1 \mu\text{M}$ and $5 \mu\text{M}$ concentrations of compound **8** on TNF- α , IL-6, 5-LOX, COX-2 and IL10 production* in LPS-stimulated RAW 264.7 cell lines. Values are mean \pm SD, $n = 3$. $P < 0.05$ vs positive control

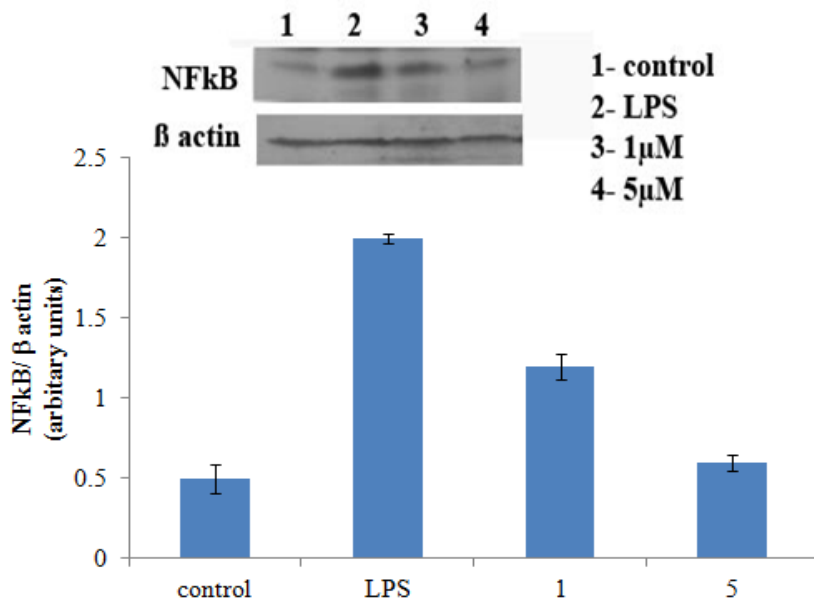


Figure S27. Western blot analysis for the expression of NF-κB in RAW 264.7 macrophages

References

Burnette WN. 1981. "Western blotting": electrophoretic transfer of proteins from sodium dodecyl sulfate--polyacrylamide gels to unmodified nitrocellulose and radiographic detection with antibody and radioiodinated protein A. *Anal Biochem* (112): 195-203.

Moshage H, Kok B, Huizenga JR, Jansen PLM. 1995. Nitrite and nitrate determinations in plasma: a critical evaluation. *Clin Chem* (41): 892-896.

Mosmann T. 1983. Rapid colorimetric assay for cellular growth and survival: application to proliferation and cytotoxicity assays. *J Immunol Methods* (65): 55-63.